Journal of Magnetic Resonance **140,** 320–324 (1999)
Article ID jmre.1999.1850, available online at http://www.idealibrary.com on IDEAL®

Single-Shot Diffusion Measurement in Laser-Polarized Gas

Sharon Peled,*,[1] Ching-Hua Tseng,*,† Aaron A. Sodickson,*,[2] Ross W. Mair,† Ronald L. Walsworth,† and David G. Cory*

*Department of Nuclear Engineering, Massachusetts Institute of Technology, 150 Albany Street, Cambridge, Massachusetts 02139; and †Harvard-Smithsonian Center for Astrophysics, Cambridge, Massachusetts 02138

Received October 7, 1998; revised April 7, 1999

A single-shot pulsed gradient stimulated echo sequence is introduced to address the challenges of diffusion measurements of laser polarized ^{3}He and ^{129}Xe gas. Laser polarization enhances the NMR sensitivity of these noble gases by $>10^3$, but creates an unstable, nonthermal polarization that is not readily renewable. A new method is presented which permits parallel acquisition of the several measurements required to determine a diffusive attenuation curve. The NMR characterization of a sample's diffusion behavior can be accomplished in a single measurement, using only a single polarization step. As a demonstration, the diffusion coefficient of a sample of laser-polarized ^{129}Xe gas is measured via this method. © 1999 Academic Press

Key Words: **hyperpolarized noble gases; ^{129}Xe; ^{3}He; bounded diffusion.**

INTRODUCTION

Optical pumping techniques can be used to transfer angular momentum from laser photons to the nuclear spins of the noble gases ^{3}He and ^{129}Xe, aligning their nuclear spin ensembles far more than in a thermal distribution (*1, 2*). This process enhances the NMR sensitivity of these gases by as much as five orders of magnitude, enabling diverse applications, including fundamental symmetry tests (*3, 4*), polarized enhancement of other species (*5, 6*), biomedical imaging (*7–9*), and gas phase diffusion measurements (*10–14*). As with imaging, diffusion measurements using laser-polarized nuclei require special consideration because the magnetization is not readily renewable. In an NMR experiment, the diffusion coefficient, D, is generally determined from a series of echo attenuation measurements following periods of diffusion in magnetization gratings (*15*). In the case of laser-polarized gases, standard NMR diffusion techniques are inefficient since the magnetization is exhausted in a single measurement before further echoes with different diffusive attenuation can be acquired. The technique described here avoids this constraint by detecting a series of echoes with different diffusive attenuation factors in a single-shot pulse sequence based on stimulated echoes. A similar sequence, based on spin-echoes, has been proposed and shown to reproduce literature values for the diffusion coefficients of a number of liquids (*16*).

The first step in measuring a diffusion coefficient is to create a magnetization grating through the application of a field gradient that winds up the phase of the transverse magnetization. In a pulsed gradient stimulated echo (PGSTE) sequence, this grating is partially destroyed by the random motion of the spins due to diffusion. Therefore, only a fraction of the initial transverse magnetization is refocused by the later application of a second field gradient, and an attenuated echo is detected. For a free gas or liquid undergoing Brownian motion, the attenuation of a grating as a function of time is an exponential decay characterized by the diffusion coefficient D. The echo amplitude is related to the rate of diffusion, the wave number of the grating $k(t)$, and the diffusion time t as

$$A = \exp\left[-D\int_0^t k^2(t')dt'\right], \qquad [1]$$

with

$$k(t) - k(0) = \gamma\int_0^t g(t')dt', \qquad [2]$$

where γ is the gyromagnetic ratio, and g is the strength of the field gradient. In the case of restricted diffusion, Eq. [1] no longer strictly applies, as the freedom of a particle's motion depends on its position in the sample. More complex models are instead necessary which involve integration of a geometry-dependent conditional displacement probability over the sample volume, with the result that the echo attenuation curve deviates from an exponential characterized by a constant diffusion coefficient. In certain circumstances, this situation may be approximated by an apparent diffusion coefficient that varies with the time scale of the measurement. Characterization of complex restricted diffusion behavior consequently requires measurement of several data points separated in time. The time

[1] Current address: Hatch NMR Center, Columbia-Presbyterian Medical Center, 710 W168th St., New York, New York 10032.

[2] Current address: Harvard-MIT Division of Health Sciences and Technology, Cambridge, Massachusetts 02139.

1090-7807/99 $30.00

dependence of the diffusion behavior then provides information about the geometry of the bounding regions.

As will be demonstrated below, the high signal-to-noise ratio of a laser-polarized sample enables the use of multiple RF excitations to generate multiple simultaneous *k*-space trajectories that produce a series of echoes from which the time-dependent diffusion behavior may be extracted regardless of the underlying physical mechanisms. The greater efficiency of this method is obtained at a cost of more complex spin dynamics. The full character of these dynamics may be straightforwardly followed via the *k*-space formalism of Ref. (*17*) as generalized in Ref. (*18*).

METHOD

While a complete description of the generalized *k*-space formalism is provided in Ref. (*18*), a brief introduction to the main points will be presented here. Under the influence of RF pulses and magnetic field gradients, the magnetization evolves as a vector field, forming spatial helices with a pitch—or spatial modulation frequency—described by a wave number k. For these experiments, the complete spin dynamics are most conveniently explored in a reciprocal space described by a Fourier decomposition basis set of right- and left-handed helices of transverse magnetization and sinusoidal amplitude modulations of longitudinal magnetization (*18*). The wave numbers $\{+k_{\text{trans}}, -k_{\text{trans}}, k_{\text{long}}\}$ describing these three basis functions may be thought of as components of a three-dimensional wave vector **k** describing the instantaneous spatial behavior of the sample. This approach leads to a set of *k*-space trajectories that fully describe the spin dynamics. That is, the spatial behavior of the spin density $\rho(x, t)$ can be tracked by following the behavior of the Fourier components of the magnetization grating as a function of time. If the initial magnetization is spatially uniform, it is described as a delta function at $k = 0$ along $\hat{z}$. Transverse magnetization is wound up into a helix by a magnetic field gradient and thus the wave vector characterizing the instantaneous magnetization grating shifts uniformly with time in a constant gradient field. In this formalism, RF pulses transfer magnetization from one basis function to another—mixing longitudinal, right-handed transverse, and left-handed transverse gratings—but they do not change the wave number, or pitch, of these modulations. Since the Fourier transform is linear, each component of the magnetization grating may be dealt with separately. In addition, the effects of RF and gradient pulses are separated in time and dealt with individually.

The single-shot pulse sequence for diffusion measurements, based on stimulated echoes, is depicted in Fig. 1. A train of small flip angle pulses—a DANTE sequence (*19–21*)—initiates *k*-trajectories that evolve under the influence of a field gradient. The spatial modulation thus formed is then projected onto the longitudinal axis by the 90° pulse in order to avoid T_2 dephasing during the long diffusion interval τ. The transverse

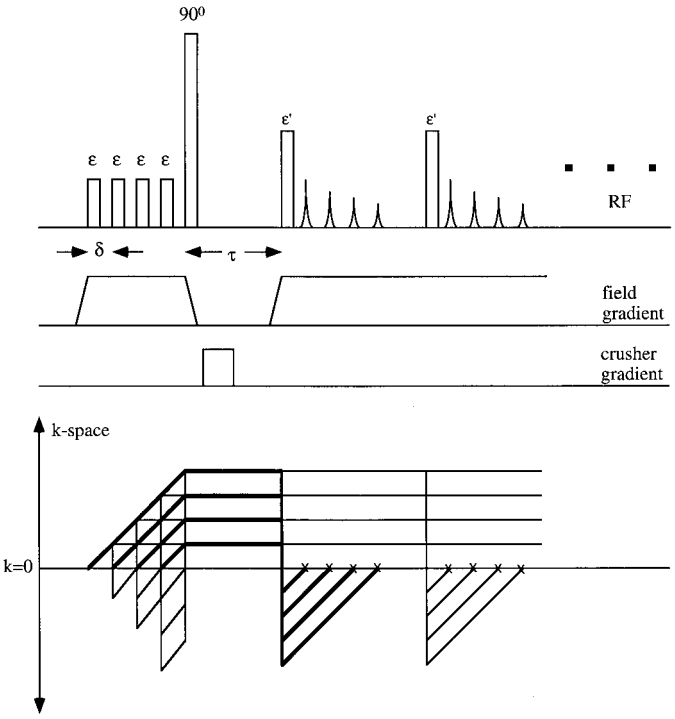

FIG. 1. Pulse sequence and *k*-space trajectories. The principle pathways in bold are the only ones to survive in the small flip angle limit and form echoes following the readout pulse. Using this sequence the full diffusive behavior of a sample can be read out in a single shot provided there is sufficient SNR. Laser-polarized gases are one example where high polarization and thus high SNR are readily achieved.

magnetization remaining after the 90° pulse is destroyed by a crusher gradient along a different axis. After a time τ, a train of stimulated echoes is recovered by a readout RF pulse of flip angle ϵ'. Given a sufficient signal-to-noise ratio, several sequential trains of stimulated echoes could be obtained with additional ϵ' pulses, each associated with different diffusion times. In this way the time dependence of the apparent diffusion coefficient D could be examined, particularly important in the case of nonexponential diffusion. Each of the main trajectories shown in boldface in Fig. 1 contributes one of the echoes and is attenuated according to Eqs. [1] and [2].

To describe the full spin dynamics of the proposed method, the initial DANTE sequence (*19*) must be explored in more detail. According to Ref. (*18*), each RF pulse ϵ transforms each wave vector of the spatial grating as:

$$\begin{bmatrix} \cos^2\left(\frac{\epsilon}{2}\right) & \sin^2\left(\frac{\epsilon}{2}\right) & \frac{1}{2}\sin(\epsilon) \\ \sin^2\left(\frac{\epsilon}{2}\right) & \cos^2\left(\frac{\epsilon}{2}\right) & \frac{1}{2}\sin(\epsilon) \\ \sin(\epsilon) & \sin(\epsilon) & \cos(\epsilon) \end{bmatrix} \begin{bmatrix} +k_{\text{trans}} \\ -k_{\text{trans}} \\ k_{\text{long}} \end{bmatrix}_{\epsilon^-} = \begin{bmatrix} +k_{\text{trans}} \\ -k_{\text{trans}} \\ k_{\text{long}} \end{bmatrix}_{\epsilon^+}. \quad [3]$$

After the first ϵ RF pulse, a transverse magnetization of amplitude $\sin(\epsilon)$ is introduced and this evolves under the gradient to a k-space offset of $k_0 = \gamma\delta g$. The longitudinal magnetization is reduced to $\cos(\epsilon)$. The second ϵ pulse:

(i) leaves the bulk of the magnetization along $\hat{z}$, with amplitude $\cos^2(\epsilon)$

(ii) introduces a new transverse magnetization component at $k = 0$, with amplitude $\cos(\epsilon) \sin(\epsilon)$

(iii) rotates part of the transverse grating at $+k_0$ back into a $\hat{z}$ grating with the same wave number k_0, with amplitude $\sin^2(\epsilon)$

(iv) rotates part of the transverse grating at $+k_0$ into a transverse grating at $-k_0$ without altering the wave number k_0, with amplitude $\sin(\epsilon) \sin^2(\epsilon/2)$

(v) leaves most of the transverse grating at $+k_0$ alone, with amplitude $\sin(\epsilon) \cos^2(\epsilon/2)$.

Therefore, immediately after the second pulse the full spatial modulation of the spin magnetization is described by the Fourier components:

longitudinal magnetization	$@k = 0$	$\cos^2(\epsilon)$	$\rightarrow 1$
	$@k = k_0$	$\sin^2(\epsilon)$	$\rightarrow 0$
transverse magnetization			
	$@k = +k_0$	$\sin(\epsilon) \cos^2(\epsilon/2)$	$\rightarrow \epsilon$
	$@k = -k_0$	$\sin(\epsilon) \sin^2(\epsilon/2)$	$\rightarrow 0$
	$@k = 0$	$\sin(\epsilon) \cos(\epsilon)$	$\rightarrow \epsilon$

which reduce to the amplitudes in the rightmost column in the limit of a small flip angle pulse ϵ. This process may be continued for later ϵ pulses, with the result that each pulse initiates a k-space trajectory of amplitude ϵ which grows in k-value under the influence of the gradient field and is essentially unaffected by later small flip angle pulses. The 90° pulse stores these gratings along $\hat{z}$ during the delay τ to avoid T_2 relaxation, while the later ϵ' pulses place a component back in the transverse plane, allowing stimulated echoes to form by evolution in the gradient field. In Fig. 1, the bold lines in k-space have magnetization amplitudes of first order in the small flip angle ϵ while the lighter lines have amplitudes of second order or higher. In the small flip angle limit, the string of stimulated echoes arise from refocusing trajectories of first order in ϵ only. These echoes attenuate to different degrees based on their different k-values and diffusion times (*18*). For the nth echo, the amplitude A_n after diffusion is

$$A_n = \exp\left[-D(\gamma g n\delta)^2 \left(\tau + \frac{2n\delta}{3} \right) \right]. \qquad [4]$$

The maximum k-value attained for the nth echo is $\gamma g n\delta$. The storage time along $\hat{z}$ contributes the term in τ to the exponent, while the initial and final sloping portions of the k-space trajectory each contribute a term in $n\delta/3$.

Continuing the analysis of the echo amplitudes as above yields a full echo amplitude for the nth echo of

$$\frac{A_n}{2} \sin(\epsilon) \sin(\epsilon') [\cos(\epsilon)]^{N-n} [\cos^2(\epsilon/2)]^{n-1}, \qquad [5]$$

where N is the total number of echoes produced by the train of N RF pulses. Each ϵ pulse applied before the nth trajectory reduces the z magnetization by $\cos(\epsilon)$, yielding the $[\cos(\epsilon)]^{N-n}$ factor. The $\sin(\epsilon)$ term arises from the RF pulse that initiates the k-space trajectory of interest, while each subsequent pulse reduces the amplitude of that trajectory by an additional factor $\cos^2(\epsilon/2)$. The 90° pulse converts the transverse magnetization helix to a sinusoid along $\hat{z}$, after which a crusher gradient eliminates the residual transverse magnetization. After the storage time τ, the ϵ' pulse restores a transverse magnetization grating, reducing the amplitude by the factor $\sin(\epsilon')/2$.

The indirect contributions to the echo amplitudes in Eq. [5] from other superimposed pathways are smaller by at least two orders in ϵ. For example, inverting a grating to a negative k-value which subsequently passes through $k = 0$ to overlap with one of the positive pathways imposes an amplitude factor of $\sin^2(\epsilon/2)$. Alternatively, sequential RF transformations from a transverse grating to a longitudinal grating and back to a transverse grating cause accumulation of amplitude factors $\sin^2(\epsilon)/2$. The amplitudes of these confounding pathways are thus easily minimized by reducing the flip angle ϵ. Taking advantage of the large SNR for laser-polarized nuclei, small flip angle pulses can be used so that the effect of these higher order k-trajectories is negligible in the determination of the diffusion behavior.

Figure 2 shows an example of the application of the single-shot technique to the measurement of unrestricted diffusion of 3 atm of isotopically enriched laser-polarized ^{129}Xe in a 25-cc cylindrical glass cell. Laser-polarization was induced using the standard spin-exchange optical pumping technique (*1*) employing infrared light (795 nm) from a fiber-coupled 15-W Optopower diode laser array projected along the ^{129}Xe-filled glass cell heated to ~90°C. The measured echo amplitudes were first corrected for the effects of nonzero flip angle RF pulses by dividing out the sine and cosine terms of Eq. [5]. Plotting the natural log of the corrected echo amplitudes against the diffusion-encoding parameter $b = (\gamma g n\delta)^2(\tau + 2n\delta/3)$ of Eq. [4] then yields a line of slope $-D$, as demonstrated in the inset of Fig. 2. The resultant diffusion coefficient $D = 0.0193$ cm^2/s is in good agreement with traditional NMR diffusion measurements on a similar sample of xenon gas when thermally polarized (*11*). In order to make measurements in spatially heterogenous porous media, for example, the SNR would have to be optimized and strong gradients used.

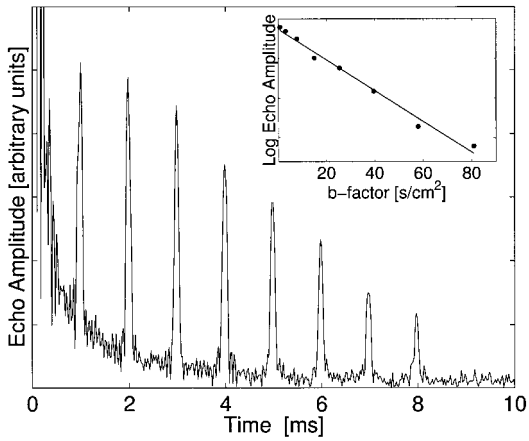

FIG. 2. Results of an eight-echo single-shot diffusion experiment with a laser-polarized ^{129}Xe sample at 3 atm gas pressure and room temperature. Inset: Plot and linear fit of echo amplitudes against the diffusion-encoding factor $b = (\gamma g n \delta)^2(\tau + 2n\delta/3)$, as defined in Eq. [4]. The slope of this linear fit yields the xenon gas diffusion coefficient $D = 0.0193$ cm^2/s, in good agreement with past measurements using other NMR techniques (*11*). The data were acquired on a GE Omega/CSI 4.7 Tesla spectrometer operating at 55 MHz for ^{129}Xe. The parameters for the pulse sequence were: flip angle $\epsilon = 6.8°$; base diffusion time, $\tau = 4.9$ ms; echo spacing $\delta = 1$ ms; readout pulse $\epsilon' = 90°$; and gradient strength $g = 1.5$ G/cm. This results in >50 spatial magnetization grating periods across the 7 cm long cylindrical cell. The inner diameter of the cell was 2 cm and the inner diameter of the RF coil was approximately 7 cm. The flip angle was calibrated separately from a train of ϵ pulses spaced 10 s apart (data not shown). Since T_1 decay is negligible for the sample over the time of the experiment, the magnetization, and hence the detected signal, is reduced only by each RF pulse.

While it is possible to work outside of the small pulse limit by calculating the amplitude of all confounding *k*-space trajectories, the additional complications are significant and the added SNR modest. One could alternatively avoid overlapping echoes from different trajectories by spacing the excitation pulses irregularly. However, for the flip angle $\epsilon = 6.8°$ used here, the amplitudes of these overlapping trajectories are less than 1% of the desired echo pathways and do not significantly alter the measured diffusive attenuation curve.

SUMMARY

A simple single-shot method is described and demonstrated for characterizing diffusion behavior. This technique is of particular value for magnetization sources that are not readily renewable, such as laser-polarized ^{3}He and ^{129}Xe. Diffusion studies of laser-polarized samples without such single-shot techniques would be quite time-consuming and for a conventional diffusion sequence would require a calibration procedure to normalize the different polarizations associated with each excitation pulse. The large magnetization available in these systems allows the acquisition of multiple measurements in a single step, thereby circumventing the time-consuming repolarization process. The technique employs multiple RF excitations to generate numerous simultaneous *k*-space trajectories that produce a series of echoes from which the diffusive behavior is determined. The complex spin dynamics that result are easily treated by the general *k*-space formalism of Sodickson and Cory (*18*).

ACKNOWLEDGMENTS

Support for this work was received from NIH Grant RO1-GM52026, NSF Grant BES-9612237, NASA Grant NAG-4920, Whitaker Foundation Grant RG 95-0228, Smithsonian Institution Scholarly Studies Program, and DOE.

Note added in proof. A related measurement of time-independent solution state ^{129}Xe diffusion may be found in (*22*).

REFERENCES

1. T. G. Walker and W. Happer, Spin-exchange optical pumping of noble-gas nuclei, *Rev. Mod. Phys.* **69,** 629–642 (1997).
2. G. Eckert, W. Heil, M. Meyerhoff, E. W. Otten, R. Surkau, M. Werner, M. Leduc, P. J. Nacher, and L. D. Schearer, A dense polarized ^{3}He target based on compression of optically pumped gas, *Nucl. Instrum. Methods A,* **320,** 53–65 (1992).
3. T. E. Chupp and R. J. Hoare, Coherence in freely precessing ^{21}Ne and a test of linearity of quantum mechanics, *Phys. Rev. Lett.* **64,** 2261–2264 (1990).
4. R. E. Stoner, M. A. Rosenberry, J. T. Wright, T. E. Chupp, E. R. Oteiza, and R. L. Walsworth, Demonstration of a two species noble gas maser, *Phys. Rev. Lett.* **77,** 3971–3974 (1996).
5. K. L. Sauer, R. J. Fitzgerald, and W. Happer, Laser-polarized liquid xenon, *Chem. Phys. Lett.* **277,** 153–158 (1997).
6. G. Navon, Y.-Q. Song, T. Room, S. Appelt, R. E. Taylor, and A. Pines, Enhancement of solution NMR and MRI with laser-polarized xenon, *Science* **271,** 1848–1851 (1996).
7. M. S. Albert, G. D. Cates, B. Driehuys, W. Happer, B. Saam, C. S. Springer Jr, and A. Wishnia, Biological magnetic resonance imaging using laser-polarized ^{129}Xe, *Nature* **370,** 199–201 (1994).
8. J. R. MacFall, H. C. Charles, R. D. Black, H. Middleton, J. C. Swartz, B. Saam, B. Driehuys, C. Erickson, W. Happer, G. D. Cates, G. A. Johnson, and C. E. Ravin, Human lung air spaces: potential for MR imaging with hyperpolarized ^{3}He, *Radiology* **200,** 553–558 (1996).
9. P. Bachert, L. R. Schad, M. Bock, M. V. Knopp, M. Ebert, T. Großmann, W. Heil, D. Hofmann, R. Surkau, and E. W. Otten, Nuclear magnetic resonance imaging of airways in humans with use of hyperpolarized ^{3}He, *Magn. Reson. Med.* **36,** 192–196 (1996).
10. G. R. Davies, T. K. Halstead, R. C. Greenhow, and K. J. Packer, High-resolution NMR of low pressure laser-polarized ^{129}Xe gas. *Chem. Phys. Lett.* **230,** 237–242 (1994).
11. R. W. Mair, D. G. Cory, S. Peled, C. H. Tseng, S. Patz, and R. L. Walsworth, Pulsed field gradient measurements of time dependent gas diffusion, *J. Magn. Reson.* **135,** 478–486 (1998).
12. B. R. Patyal, J-H. Gao, R. F. Williams, J. Roby, B. Saam, B. A. Rockwell, R. J. Thomas, D. J. Stolarski, and P. T. Fox, Longitudinal relaxation and diffusion measurements using magnetic resonance signals from laser-hyperpolarized ^{129}Xe nuclei, *J. Magn. Reson.* **126,** 58–65 (1997).

13. M. Bock, Simultaneous T_2^* and diffusion measurements with ^{3}He, *Magn. Reson. Med.* **38,** 890–895 (1997).

14. D. M. Schmidt, J. S. George, S. I. Penttila, A. Caprihan, and E. Fukushima, Diffusion imaging with hyperpolarized ^{3}He gas, *J. Magn. Reson.* **129,** 184–187 (1997).

15. P. T. Callaghan, *Principles of nuclear magnetic resonance microscopy,* Oxford Science, Oxford, 1991.

16. S. J. Doran and M. Décorps, A robust, single-shot method for measuring diffusion coefficients using the "Burst" sequence, *J. Magn. Reson. Ser. A,* **117,** 311–316 (1995).

17. J. Hennig, Multiecho imaging sequences with low refocussing flip angles, *J. Magn. Reson.* **78,** 397–407 (1988).

18. A. A. Sodickson and D. G. Cory, A generalized k-space formalism for treating the spatial aspects of a variety of NMR experiments, *Prog. NMR Spectr.* **33,** 77–108 (1998).

19. G. A. Morris and R. Freeman, Selective excitation in fourier transform nuclear magnetic resonance, *J. Magn. Reson.* **124,** 433–462 (1978).

20. L. Zha and I. J. Lowe, Optimized ultra-fast imaging sequence (OUFIS), *Magn. Reson. Med.* **33,** 377–395 (1995).

21. J. Hennig and M. Hodapp, Burst imaging, *MAGMA* **1,** 39–48 (1993).

22. J. Wolber, S. J. Doran, M. O. Leach, and A. Bifone, Measuring diffusion of xenon in solution with hyperpolarized ^{129}Xe NMR, *Chem. Phys. Lett.* **296,** 391–396 (1998).